Chapter-V

DC Conductivity Studies

This chapter deals with the dc conductivity results of three different series which explains in detail the temperature and composition dependence of dc conductivity. Hopping mechanism in electronic conducting samples is discussed on the basis of Mott's Model.

5.1 Introduction:

Electrical properties of glasses have been studied extensively for a number of years due to their potential use in solid state devices. Glasses containing large amount of transition metal ions (TMI), such as Fe, Co, Mo, W, V etc., are known to be electronic semiconductors [1, 2]. Electrical properties of these glasses are determined by the presence of TMI in two different valance states [3, 4], for example, V^{+4} and V^{+5} states in vanadium glasses and Fe^{+2} and Fe^{+3} in iron-based glasses. Various binary or ternary glass systems have been synthesized using B_2O_3, P_2O_5 and TeO_2 as network forming oxides and alkali or silver oxides as network modifiers. In systems containing alkali oxides, ionic conduction along with electronic conduction contributes in electrical conduction process and the system will be termed as mixed (electronic-ionic) conductor. In these glasses, 'crossover' from predominantly electronic to ionic conductivity can result from composition dependence. Ionic conduction is due to the motion of the silver or alkali ions [5]. Transport of oxide ions occurs generally by hopping process between an occupied and vacant oxide ion site [6, 7].

The glasses in the Ag_2O-V_2O_5-TeO_2 system are particularly interesting as they show high electronic conductivity up to 10^{-5} Ω^{-1} cm^{-1} at room temperature [8-10]. In that case, electrical conductivity is found to be purely electronic with a polaronic hopping conduction mechanism. Glasses with low concentration of transition metal oxide and a high concentration of alkali or silver oxides are well known as super ionic conductors [5]. Purely ionic conducting glasses can be used as solid electrolytes, and those exhibiting mixed conduction can be employed as cathode materials in novel advanced electrochemical cells.

In the present work, glass samples are prepared using V_2O_5 and TeO_2 as network formers and BaO and Ag_2O as network modifiers. It is reported that [11] on adding Ba ions, the electronic paths are progressively blocked, causing a decrease in electronic conductivity because Ba ion acts as glass modifiers. It will create non-bridging oxygen (NBO) and break the glass network. When we substitute Ag_2O in this barium vanadate tellurium oxide glass system, it exhibits mixed conductivity. The Ag^+ ions act as charge carriers in this glass system while the electronic conductivity is exhibited due to the presence of vanadium pentoxide.

The electrical conductivity (σ) of the glasses was determined by

$$\sigma = \frac{1}{R}\left(\frac{t}{A}\right) \qquad \text{.....(5.1)}$$

where t is the thickness, A is the area and R is the resistance of the glass samples. Electrical conductivity studies have been carried out on the following series of the glass samples at different temperature range.

1) x (BaO : 1.5 Ag_2O) - (95-x) V_2O_5 – 5 TeO_2;

   where x = 25, 30, 35, 40, 45.

2) 10 BaO-y Ag_2O-(85-y) V_2O_5-5 TeO_2;

   where y = 20, 25, 30, 35, 40, 45, 50, 55.

3) 5 BaO-z Ag_2O-35 V_2O_5- (60-z) TeO_2;

   where z = 25, 30, 35, 40, 45, 50, 55, 60.

5.2 Temperature dependence of DC Conductivity:

The dc conductivity studies of semiconducting glasses with transition metal oxides have galvanized numerous studies on vanadate glasses worldwide [12, 13,

14]. The logarithm of dc conductivity versus 1000/T for all compositions of three different series are shown in Figure 5.1 (a), (b) and (c) from room temperature to below the glass transition temperature. These plots follow the Arrhenius behavior of the form

$$\sigma_{dc} = \sigma_0 \exp\left(\frac{-W}{kT}\right) \qquad \text{.....(5.2)}$$

where σ_{dc} is the dc conductivity, σ_0 is the pre exponential factor, k is the Boltzmann constant and W is the activation energy which is calculated by least square straight line fitting of log σ_{dc} versus 1000/T plot for all the samples.

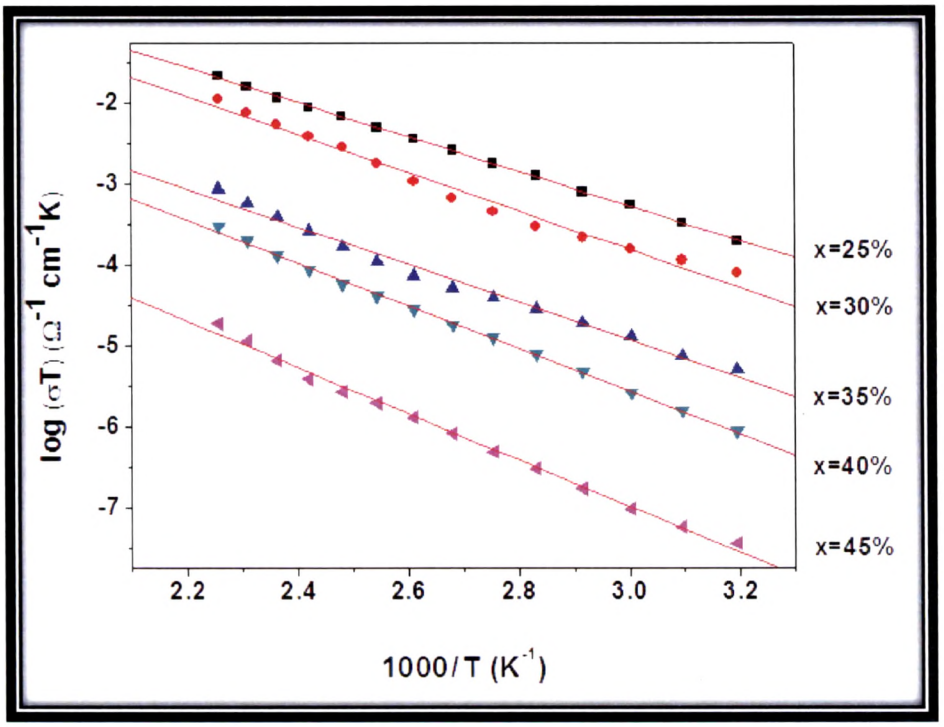

Fig. 5.1 (a): log (σT) versus 1000/T for first series samples.

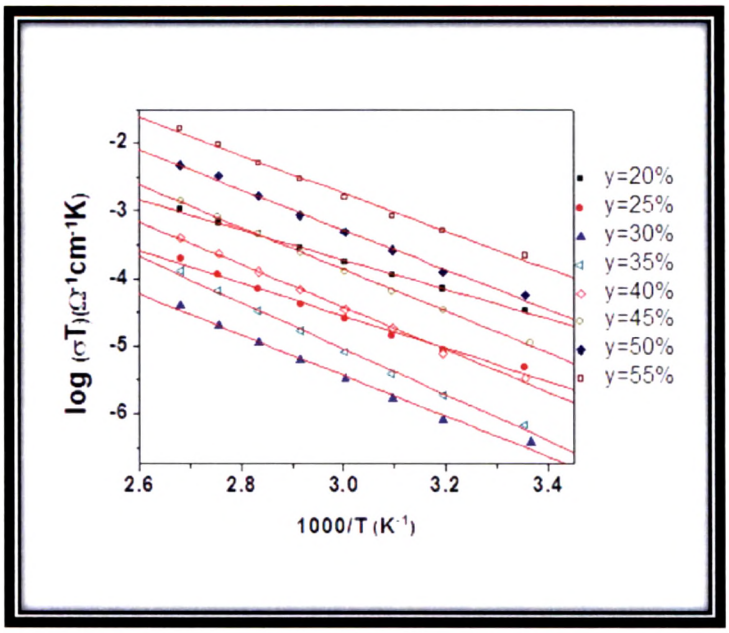

Fig. 5.1 (b): log (σT) versus 1000/T for second series samples.

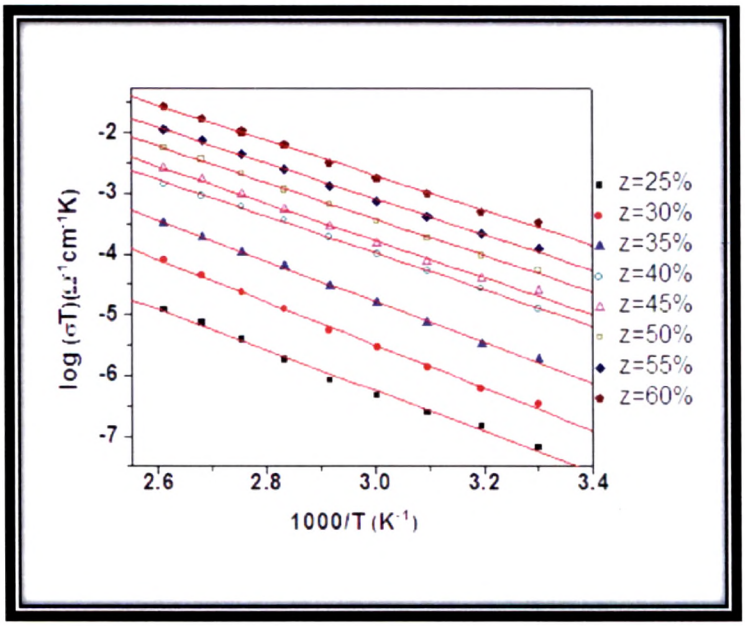

Fig. 5.1 (c): log (σT) versus 1000/T for third series samples.

Table.5.1: Activation energy of glass samples of three different series.

First series		Second series		Third series	
x (mol%)	W(eV)	y (mol%)	W(eV)	z (mol%)	W(eV)
25	0.39	20	0.41	25	0.63
30	0.40	25	0.45	30	0.67
35	0.43	30	0.58	35	0.63
40	0.48	35	0.65	40	0.60
45	0.52	40	0.60	45	0.58
		45	0.59	50	0.57
		50	0.56	55	0.55
		55	0.53	60	0.54

Variation of conductivity with temperature is observed in all the three series which shows the semiconducting behavior of all glass samples. The plots for all compositions are linear, indicating thermally activated hopping conductivity. The calculated values of activation energy are shown in Table.5.1 for all the three series. The general behavior of the curves are similar to that reported for V_2O_5-P_2O_5 glasses [15, 16, 17], V_2O_5-TeO_2 [18], WO_3-P_2O_5 [19], V_2O_5-B_2O_3 glasses [20].

5.3 Compositional dependence of DC Conductivity:

Glass modifier plays a very important role in the glass formation and also has characteristics to change the properties of glasses like electrical conductivity, switching etc. The dependence of conductivity on the modifier content has also been studied by many workers [21, 22, 23].

The variation of σ_{dc} and activation energy with the modifier content ($BaO:1.5Ag_2O$) in the first series is shown in Fig. 5.12(a) when it is measured at zero frequency value in a complex impedance plot. Figure shows that σ_{dc} decreases continuously except at x=30 mol% where its value is slightly high while the activation energy increases except for x=30 mol% sample, at which its value is slightly low. DC conductivity of the glass samples of first series is also measured by applying constant current and measuring voltage drop across the sample. The dc conductivity and activation energy calculated in this way is plotted against modifier content in Fig. 5.12(b). Here in this figure, it is clear that conductivity decreases while the activation energy increases with increasing modifier content.

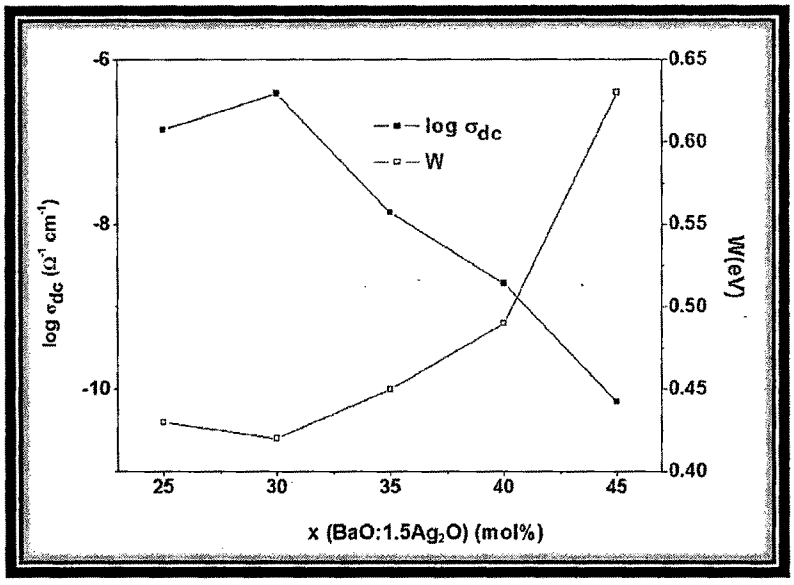

Fig. 5.12 (a): Variation of σ_{dc} and activation energy W(eV) with modifier content for first series.

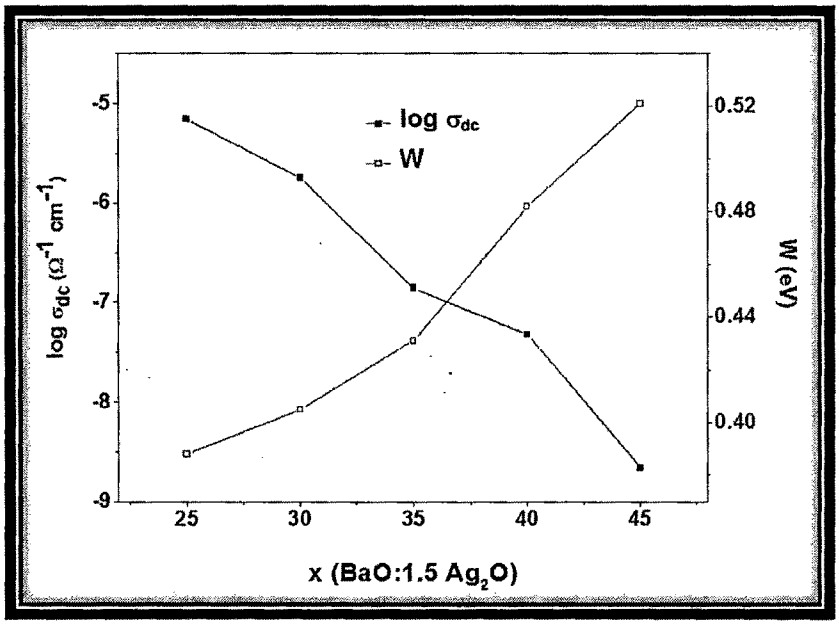

Fig. 5.12 (b): Variation of σ_{dc} and activation energy with modifier content for first series (DC Method).

It has been previously reported [24, 25] that in vanadate glasses the dc conductivity is electronic due to the presence of vanadium in different valence state and depends strongly upon the average distance R_V between the vanadium ions. As the modifiers are introduced into the vanado-tellurite network, they are supposed to go into network at interstitial position and break the network of vanadium and tellurium. Because of the breaking of V_2O_5 structure, the atomic site spacing between V-V increases. The average distance $(R_{V\text{-}V})$ was calculated for the present glasses by Eq.2.26, where N_V is the concentration of vanadium ions per unit volume, calculated from batch composition and the measured density (Eq.2.28). These calculated values of N_V and R_V are given in Table.5.2. It is clear from the Table that due to the addition of modifier (BaO and Ag_2O), the distance between vanadium ions increases i.e., R_V increases. Assuming that the conductivity is due to electron hopping from V^{+4} to V^{+5} then with increasing R from 0.39 nm to 0.42 nm , it is reasonable to expect a decrease in dc conductivity. At the same time, the activation energy appears to increase with increasing distance between the vanadium ions i.e., R_V. The decrease in conductivity is also evident from the transport number study of this series where the value $(t_e\text{-}t_{Ag})$ decreases continuously with increasing modifier indicating that the electronic component is dominating in the series and its value continuously decreases with modifier. Hence, the resulting effect of the present composition in first series is to decrease the conductivity and increase of the activation energy with the increasing amount of glass modifier.

Mott's theory of conductivity in semiconducting oxide glasses suggests that the dc conductivity is controlled by electron hopping and depends upon the distance R_V, between the vanadium ions in first series samples which is also clear by the small

value of activation energy (0.39 eV) for 25 mol % glass sample. As it is known, that if the polaron radius is less than the interatomic distance R_V (i.e., $r_p < R_V$) then the polaron is said to be "small polaron". Thus, to confirm the small polaron existence in our case, we have calculated the polaron radius from the Eq.2.27. The calculated value of polaron radius increases from 0.157 nm to 0.167 nm with increasing modifier (Table.5.2). These small values of polaron radius suggest that the polarons are highly localized. The density of states $N(E_f)$ is also estimated [26] from

$$N(E_f) = \frac{3}{4}\pi R_V^3 W \qquad \text{.....(5.3)}$$

The calculated values of density of states $N(E_f)$ ranges from 10.41 × 10^{21} to 6.41 × 10^{21} eV^{-1} cm^{-3} as listed in Table.5.2. These obtained values for the present systems are reasonable to indicate localized states and are quite similar to the values of other systems based on vanadium for e.g., (3.79-10.49 × 10^{21} eV^{-1} cm^{-3}) for V_2O_5-Fe_2O_3-TeO_2 [27] and (3.75-12.4 × 10^{21} eV^{-1} cm^{-3}) for BaO-V_2O_5 system [28].

Another important polaronic parameter is the small polaron coupling constant ν_p, which is a measure of electron phonon interaction and is given by

$$\nu_p = \frac{2W_h}{h\nu_0} \qquad \text{.....(5.4)}$$

Usually, the values of $\nu_p > 4$, indicate a strong electron phonon interaction [26]. The estimated values of ν_p, in our case, lie in between 13.39 to 12.36, as shown in Table.5.2. These values are larger in comparison with V_2O_5-Bi_2O_3 glasses doped with $BaTiO_3$, in which its range is 7.05 to 7.6 [29]. The polaron hopping energy W_h was calculated by Eq.2.25, using the approximation $\varepsilon_p \approx \varepsilon_\infty = n^2$, where n is the

Table.5.2: Some physical parameters of the glass system for first series.

x (mol%)	N_v ($\times 10^{22}$ cm^{-3})	$R_{V\text{-}V}$ (nm)	r_p (nm)	$N(E_f)$ ($\times 10^{21}$ eV^{-1} cm^{-3})	ν_p
25	1.69	0.390	0.157	10.4	13.39
30	1.61	0.396	0.160	9.49	13.11
35	1.55	0.400	0.162	8.60	12.89
40	1.47	0.408	0.164	7.29	12.62
45	1.40	0.415	0.167	6.41	12.36

Table.5.3: Some physical parameters of first series glass samples.

x (mol%)	W_h (eV)	ε_p	log σ_0 (Ω^{-1} cm^{-1})
25	0.28	4.92	3.08
30	0.27	4.96	2.86
35	0.27	4.98	2.32
40	0.26	5.00	2.23
45	0.26	5.02	1.39

refractive index of the glass [30]. At present, the standard values of the refractive index of $BaO\text{-}Ag_2O\text{-}V_2O_5\text{-}TeO_2$ glasses are not available. In order to obtain these values we use $n = \sum c_i n_i$, where c_i and n_i are the concentrations and refractive indices of the component oxides of the studied glasses. The calculated values of W_h (polaron hopping energy) and ε_p (effective dielectric constant) are given in Table 5.3. The log σ_0 (logarithm of pre-exponential factor) was obtained from the extrapolation of the straight portion of the log (σT) against $1000/T$ curve, shown in Fig.5.1.(a). The variation of the values of log σ_0 with modifier is given in Table.5.3. This confirms that the non-adiabatic hopping conduction occurs in the present glass system. As for the non-adiabatic hopping conduction, the term σ_0 (pre exponential factor) should depend on composition [28, 31].

In the second series $10\ BaO\text{-}yAg_2O\text{-}(85\text{-}y)V_2O_5\text{-}5TeO_2$; BaO and TeO_2 are kept constant at 10 and 5 mol % respectively while the amount of Ag_2O increases from 20 to 55 mol% and vanadium decreases from 65 to 30 mol %. Fig 5.13, shows the variation of conductivity and activation energy with Ag_2O mol % which clearly shows that for the first three samples i.e., y=20, 25 and 30 mol%, conductivity decreases with increasing Ag_2O while for the samples y=35, 40, 45, 50, 55 mol%, conductivity starts increasing with increasing Ag_2O content. This suggests a changeover from predominantly electronic to ionic conductivity. The activation energy increases from 0.41 eV (for y=20 mol %) to 0.65 eV (for y=35 mol% sample) and after that it decreases. Usually, the lowest conducting sample has the highest activation energy or vice versa [32] but in our case, 30 mol% shows lowest conductivity and 35 mol% shows highest activation energy, may be due to the reason that the sample having modifier between 30 and 35 mol% might be the

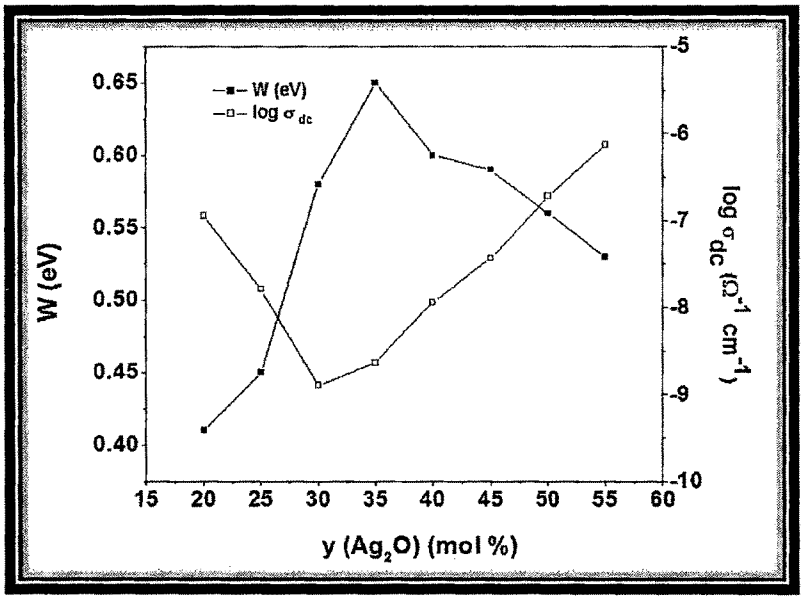

Fig 5.13: Variation of σ_{dc} and activation energy with Ag_2O mol % for second series.

lowest conducting sample. The minima of conductivity on composition have been observed for glasses of other systems also such as Li_2O-WO_3-P_2O_5 [33], Na_2O-V_2O_5-TeO_2 [34], Li_2O-MoO_3-P_2O_5 [5], Li_2O-V_2O_5-P_2O_5 [35], Ag_2O- V_2O_5-TeO_2 [36]. There can be atleast two reasons for the presence of such minima. The most natural is the decrease of electronic conductivity at the expense of the ionic one [34]. In this case, electronic and ionic currents are independent of each other. According to Bazan et. al., [33], the presence of minima is due to direct coupling between electronic and ionic fluxes, caused by the electrostatic interactions between mobile ions and electrons (polarons). The argument is that the mobile electrons (or polarons) formed by the capture of the moving electron by a V^{+4} atom are attracted towards the oppositely charged Ag^+ ions. This so formed cation-polaron pair tends to move together as a neutral entity. The migration of

Table.5.4: Some physical parameters of second series glass samples.

y (mol%)	N_V ($\times 10^{22}$ cm^{-3})	$R_{V\text{-}V}$ (nm)	N_{Ag} ($\times 10^{22}$ cm^{-3})	$R_{Ag\text{-}Ag}$ (nm)	log σ_0 (Ω^{-1} cm^{-1})
20	1.62	0.39	0.50	0.59	2.88
25	1.55	0.40	0.65	0.54	2.75
30	1.49	0.41	0.81	0.50	3.59
35	1.37	0.42	0.96	0.47	5.17
40	1.28	0.43	1.14	0.44	5.04
45	1.17	0.44	1.32	0.42	5.44
50	1.08	0.45	1.55	0.40	5.58
55	0.95	0.47	1.75	0.38	5.67

Table.5.5: Polaronic hopping parameters for electronic conducting glasses in second series.

y (mol%)	r_p (nm)	$N(E_f)$ ($\times 10^{21}$ eV^{-1} cm^{-3})	ν_p	W_h (eV)	ε_p
20	0.159	9.44	13.02	0.27	5.01
25	0.162	8.24	12.67	0.26	5.08
30	0.164	6.15	12.34	0.25	5.14

these pairs does not involve any net displacement of electric charge so this process will contribute nothing to the electrical conductivity. When sufficient Ag^+ ions are present, the movement of free cations is greater than the movement of free polarons and hence, the cationic conductivity will once again increases with Ag_2O content. Barczynski et. al. [4] have suggested that by the internal friction method, it is possible to observe the relaxation of neutral ion-polaron pairs.

Another interpretation would be to assume simple independent ionic and electronic paths in the glass. An electronic path would consist of a continuous electronic transferring along a chain, in which V^{+4} and V^{+5} are regularly disposed. An ionic path would be made by a regular disposition of non-bridging oxygen along the network former chains allowing the interstitial pair displacement. On adding Ag_2O in the system, the spacing between vanadium ions ($R_{V\text{-}V}$) increases, as shown in Table.5.4. At the same time, the jump distance for the Ag^+ ions decreases and the introduction of non-bridging oxygen facilitates their hopping. Thus, the electronic paths are progressively blocked causing the electronic conduction to fall down. The $R_{Ag\text{-}Ag}$ and N_{Ag} values are calculated by Eq.2.26 and Eq.2.28 respectively where F_W and M_W are the weight fraction and molecular weight of Ag_2O respectively. These values are given in Table.5.4.

In the TeO_2 based glasses, from the ionic conductivity point of view, the transformation from TeO_4 to TeO_3 is important because this transition involves a continuous formation of non-bridging oxygen (NBOs) which are responsible for the changes in conductivity [37]. In the present system, it is clear from IR studies (Fig. 4.22) that above y=35 mol % sample, TeO_3 (peak at 777 cm^{-1} is assigned to TeO_3 group) groups are formed and below 35 mol % sample TeO_4 polyhedra are present. Thus, we can say that there is a transition from TeO_4 to TeO_3 with the

addition of Ag_2O which may be the reason for the increase in conductivity. E. Sanchez et.al. [38, 39] have also marked electronic to ionic conductivity switchover in Li_2O-TeO_2-V_2O_5 glass system and explained the increase in terms of optical basicity according to Li_2O content, diminishing the amount of polaron conductivity and favoring ionic conductivity as Li_2O went up to higher concentration. Hence, in the second series, the whole shape of the curve for isothermal conductivity can be seen as the intersect of two curves corresponding to electronic and ionic conductivities, respectively and the relative minimum as corresponding to the change of mechanism for the electrical transport process.

For the samples, showing dominating electronic conductivity i.e., y=20, 25 and 30 mol%, the polaronic parameters have been calculated, as shown in Table.5.5. The polaron radius (r_p) calculated from Eq.2.27 varies from 0.159 nm to 0.164 nm with increasing Ag_2O content. These values suggest that the polarons are highly localized and it can be seen that the requirement of applying small polaron theory i.e., $r_p < R$ are fulfilled in our case. The density of state $N(E_f)$ values vary from 9.44×10^{21} to 6.15×10^{21} eV^{-1} cm^{-3} and the values are reasonable to show localized states. The small polaron coupling constant γ_p lies in between 13.02 to 12.34 as shown in Table.5.5 which also indicates strong electron phonon interaction. The polaron hopping energy (W_h) calculated from Eqn.2.25 (chapter 2), decreases from 0.27 to 0.25 eV with increasing modifier content in this series and the values are given in Table 5.5. The effective dielectric constant ε_p values that are used for calculating polaron hopping energy are also given in Table.5.5 for the samples showing polaronic conductivity. Pre-exponential factor (Table.5.4), obtained from the extrapolation of the straight line portion of the plot

log (σT) versus 1000/T, for all samples of second series, clearly shows that it depends on composition, indicating non-adiabatic hopping for electronic conducting samples. Table 5.4 also shows that the calculated values of pre-exponential factor for electronic conducting region ($20 \leq x \leq 30$) are lower than those for ionic conducting region ($35 \leq y \leq 55$). Similar results are also obtained for other glass systems of different compositions [40]. The decrease in polaronic conductivity from y=20 to 30 mol% is also evident from Fig. 4.25, where electronic transport number (t_e) dominates over silver ion transport number (t_{Ag}) and (t_e-t_{Ag}) value decreases from 20 to 30 mol% samples above which silver ion transport number is dominating and conductivity increases with further addition of Ag_2O in the system.

In the third series 5 BaO-z Ag_2O-35 V_2O_5- (60-z) TeO_2; BaO and V_2O_5 are kept constant at 5 mol % and 35 mol% respectively while Ag_2O increases from 25 to 60 mol% and TeO_2 decreases from 35 to 0 mol %. Fig.5.14 shows the variation of conductivity and activation energy with Ag_2O mol % for third series. The conductivity of the samples increases continuously and the highest conducting sample shows the lowest activation energy because the ions in that sample have to overcome the smallest energy barrier while conducting [32].

The addition of metal oxide Ag_2O to the glass formers involves incorporation of oxygen into macromolecular chain formed by the network formers V_2O_5 and TeO_2, thereby introducing ionic bonds in the glass system. As the modifier increases, greater numbers of oxygen bridges are broken. The increasing non-bridging oxygen in the system decreases the length of the macromolecular chains. So the increasing addition of modifier breaks the bond and facilitates easy

migration of the conducting ions. When Ag_2O increases in the system, spacing between vanadium ions increases (Table.5.6) while that of Ag^+ decreases ($R_{Ag\text{-}Ag}$) and the introduction of non-bridging oxygen facilitates their hopping. The calculated values of Ag^+ ion concentration (N_{Ag}) and jump distance ($R_{Ag\text{-}Ag}$) for all

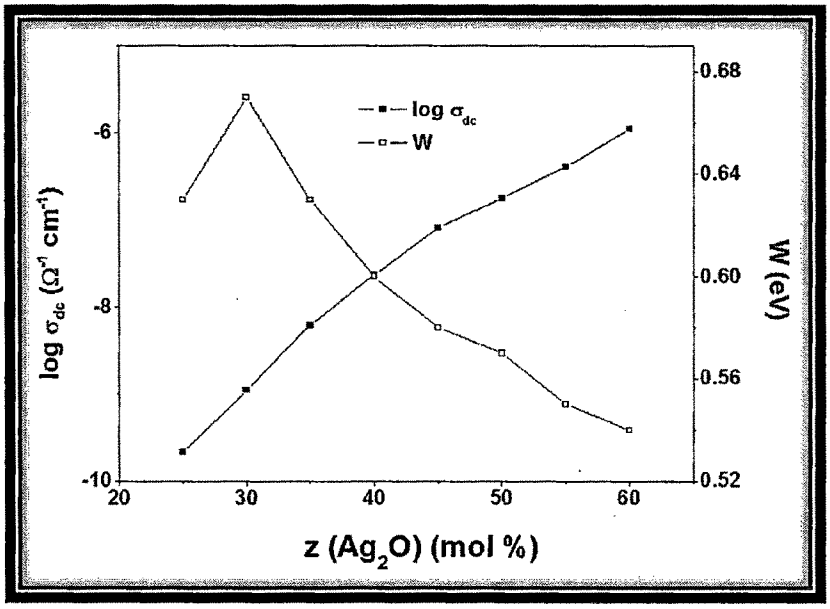

Fig. 5.14: Variation of σ_{dc} and activation energy with Ag_2O mol % for third series.

the samples are given in Table.5.6. This increasing number of non-bridging oxygens with silver content is supported by the decrease in the glass transition temperature (Figs.4.17 & 4.19) with silver oxide content [41, 42].

It is also reported that, when alkali oxides are introduced into the tellurite network, different structural units are formed at different alkali oxide contents [43, 44, 45, 46]. Similar to alkali tellurite glasses, silver tellurite glasses also exhibit

Table.5.6: Some physical parameters of third series glass samples.

z (mol%)	N_V ($\times 10^{22}$ cm^{-3})	$R_{V\text{-}V}$ (nm)	N_{Ag} ($\times 10^{22}$ cm^{-3})	$R_{Ag\text{-}Ag}$ (nm)
25	1.05	0.457	0.75	0.51
30	1.06	0.456	0.90	0.48
35	1.07	0.454	1.07	0.45
40	1.07	0.454	1.22	0.43
45	1.07	0.454	1.37	0.42
50	1.08	0.453	1.54	0.40
55	1.08	0.453	1.69	0.39
60	1.07	0.455	1.83	0.38

structural transition from TeO_4 trigonal bipyramids to TeO_3 trigonal pyramids through TeO_{3+1} polyhedra with increasing silver oxide content [47, 48]. The transition from TeO_4 to TeO_3 is also confirmed from the FTIR spectra (Fig.4.23) and the formation of TeO_3 polyhedra with the increase of Ag_2O, might be responsible for the increase in conductivity and facilitating the ease in transport of Ag^+ ions in the glass matrix.

The similar variations of conductivity as a function of alkali content have been reported in other ternary glass systems also [40, 34, 33, 49, 50]. The transport number study by the EMF method also supports the increase in conductivity with the addition of Ag_2O (Fig. 4.26 and Table.4.1).

5.4 Nature of hopping process:

The nature of hopping mechanism [51, 15] can be ascertained by the plot of log σ_{dc} versus W at an arbitrary chosen experimental temperature. If it gives a slope of line equal to (1/2.303 kT), the hopping is adiabatic in nature. If it differs from the said value, non-adiabatic approximation can be considered. The similar plot is shown for the samples of the first and second series in which polaronic conduction dominates. In the first series plot, shown in Fig. 5.15, the estimated temperature from the slope is 201.34 K and the experimental temperature is 353 K. As the estimated temperature is different from the chosen temperature, the term exp(-$2\alpha R$) contributes to the conductivity and non-adiabatic hopping is confirmed. Sakata and co-workers have studied the electrical properties, mainly on the dc conductivity of many ternary vanadium-tellurite glasses, V_2O_5-TeO_2-R, where the third component R=Sb [31], Sb_2O_3, SnO, Bi_2O_3, ZnO, NiO or PbO [52-57]. It is

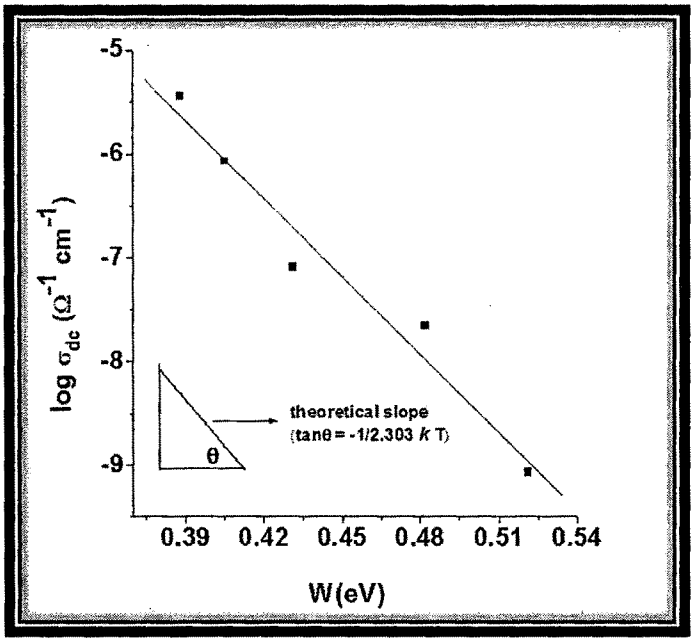

Fig.5.15. Plot of W versus log σ_{dc} at temperature 353 K for first series.

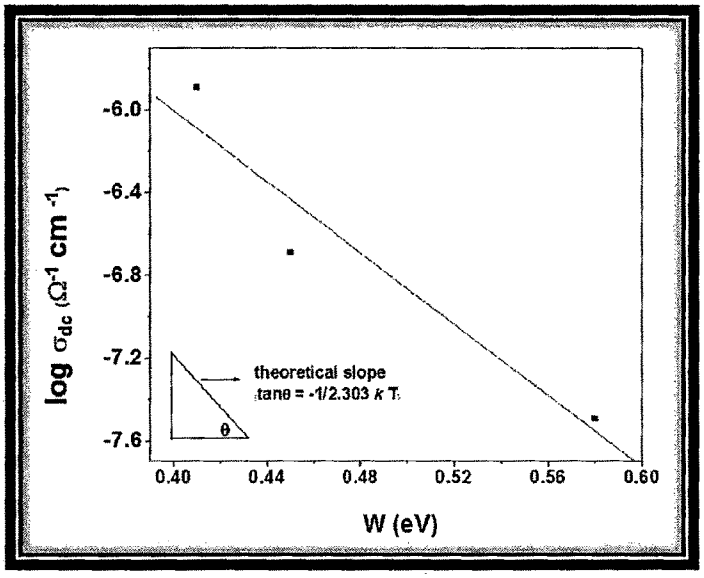

Fig.5.16. Plot of W versus log σ_{dc} at temperature 353 K for second series.

found that the electrical conduction is due to the adiabatic small polaron for V_2O_5 $\geq$ 50 mol % and is non-adiabatic for $V_2O_5 \leq$ 50 mol %, whereas in our case it is non-adiabatic for $V_2O_5 >$ 50 mol%.

Similar plot for second series at 353 K for y=20, 25 and 30 mol % samples is shown in Fig. 5.16. Here, the temperature estimated from the slope of the figure is 586 K which is quite different from the experimental temperature i.e., 353 K which attributes non-adiabatic nature of hopping in these samples.

References:

[1] G. B. Devidas, T. Sankarapa, B. K. Chougule, G. Prasad, J. Non-Cryst. Solids 353 (2007) 426-434.

[2] L. Murawski, R. J. Barczynski, Solid State Ionics 176 (2005) 2145-2151.

[3] B. Dutta, N. A. Fahmi, I. L. Pegg, J. Non-Cryst. Solids 351 (2005) 1958-1966.

[4] R. J. Barczynski, L. Murawski, Mat. Sci. Poland 24 (1) (2006) 221.

[5] L. Bih, M. El. Omari, J. M. Reau, M. Haddad, D. Boudlich, A. Yacoubi, A. Nadiri, Solid State Ionics 132 (2000) 71-85.

[6] V. Thangadurai, W. Weppner, Ionics 12 (2006) 81-92.

[7] K. J. Rao, "Structural chemistry of glasses", 1st edn. Elsevier Science, Amsterdam, pp. 203-262.

[8] B. W. Flynn, A. E. Owen, and J. M. Robertson, p. 678 in *Proceedings of the 7th Conference on Amorphous and Liquid Semiconductors,* CICL, University of Edinburgh, Edinburgh, Scotland, 1977.

[9] V. K. Dhawan and A. Mansingh, J. Non-Cryst. Solids **51**, 87–103 (1982).

[10] N. Chopra, A. Mansingh, and G. K. Chadha, J. Non-Cryst. Solids **126**, 194–201(1990).

[11] S. Szu, Fu-Shyang Chang, Solid State Ionics 176 (2005) 2695-2699.

[12] K. Shimakawa, Philos. Mag. 60 (1989) 377.

[13] H. Hirashima, M. Mitsuhasi and T. Yoshida, Yogo-Kyokai-Shi 90 (1982) 411.

[14] H. Hirashima, H. Kurokawa, K. Mizobuchi and T. Yoshida, Glastech. Ber. 61 (1988) 151.

[15] M. Sayer, A. Mansingh, Phys. Rev. B, 6 (1972) 4629.

[16] M. Sayer, A. Mansingh, J. M. Reyes and G. Rosonblatt, J. Appl. Phys. 42 (1971) 2857.

[17] G. S. Linsley, A. E. Owen and F. M. Hayatee, J. Non-Cryst. Solids 85 (1986) 170.

[18] Y. Dimitriev and V. Dimitriev, Mater. Res. Bull. 13 (1978) 1071.

[19] A. Mansingh, A. Dhawan, R. P. Tandon and J. K. Vaid, J. Non-Cryst. Solids 27 (1978) 309.

[20] E. Culea, Al. Nicula, Solid State Communications 58 (1986) 545-549.

[21] Hirashi Hirashima, Daikichi Arai, Tetsuro Yoshida, J. Am. Ceram. Soc. Vol. 68. No. 9 (1985) 486-489.

[22] B. K. Sharma, D. C. Dubey, A. Mansingh, J. Non-Cryst. Solids, 65 (1984) 39.

[23] M. M. Ahmed, C. A. Hograth, J. Mater. Sci. 18 (1983) 3305.

[24] M. M. El-Desoky, J. Mater. Sci. Mater. Electron. 14 (2003) 215.

[25] S. Sen, A. Ghosh, J. Appl. Phys. 86 (1999) 2078.

[26] N. F. Mott, E. A. Davis, Electronic Processes in Non-Crystal Materials, Clarendon Press, Oxford, 1979.

[27] M. M. Desoky, J. Non-Cryst. Solids 351 (2005) 3139-3146.

[28] A. Al-Hajry, A. Al-Shahrani, M. M. El-Desoky, Mat. Chem. Phys. 95 (2006) 300-306.

[29] A. Ghosh, J. Appl. Phys. 66 (1989) 2425.

[30] H. El Mkami, B. Deroide, R. Backov, J. V. Zanchetta, J. Phys. Chem. Solids 61 (2000) 819-826.

[31] H. Mori, H. Matsuno, H. Sakata, J. Non-Cryst. Solids 276 (2000) 78-94.

[32] H. X. Wang, Z. X. Wang, H. Li, Q. B. Meng, L. Q. Chen, Electrochim Acta

52 (2007) 2039-2044.

[33] J. C. Bazan, J. A. Duffy, M. D. Ingram, and M. R. Mallace, Solid State Ionics, 86– 88, 497–501 (1996).

[34] G. D. L. K. Jayasinghe, M. A. K. L. Dissanayake, M. A. Careem, and J. L. Souquet, Solid State Ionics, 93, 291–295 (1997).

[35] J. E. Garbarczyk, M. Wasiucionek, P. Jozwiak, L. Tykarski, J. L. Nowinski, Solid State Ionics 154 (2002) 367-373.

[36] H. M. M. Moawad, H. Jain, R. El-Mallawany, J. Phys. Chem. Solids 70 (2009) 224-233

[37] B. V. R. Chowdari, P. Kumari, Solid State Ionics 113-115 (1998) 665.

[38] E. Sanchez, C. A. Angell, Mater. Res. Soc. Symp. Proc., 548 (1999) 461-466.

[39] E. Sanchez, L. Torres-Martinez, C. A. Angell, Bol. Soc. Esp. Ceram. Vidr. 40(2) (2001) 125-129.

[40] G. D. L. K. Jayasinghe, M. A. K. L. Dissanayake, P. W. S. K. Bandaranayake, J. L. Souquet, D. Foscallo, Solid State Ionics 121 (1999) 19-23.

[41] A. Pan, A. Ghosh, Phys. Rev. B. 59 (1999) 899-904.

[42] C. S. Sunandana, T. Kumaraswami, J. Non-Cryst. Solids 85 (1986) 247-250.

[43] T. Sekiya, N. Mochida, A. Ohtsuka, M. Tonokawa, J. Non-Cryst. Solids 144 (1992) 128.

[44] S. Sakida, S. Hayakawa, T. Yoko, J. Non-Cryst. Solids 243 (1999) 13.

[45] H. Munemura, K. Mitome, M. Misawa, K. Maruyama, J. Non-Cryst. Solids 293-295 (2001) 700.

[46] J. C. McLaughlin, S. L. Tagg, J. W. Zwanziger, J. Phys. Chem. B 105 (2001) 67.

[47] J. Dexpert-Ghys, B. Piriou, S. Rossignol, J. M. Reau, B. Tanguy, J. J. Videau, J. Portier, J. Non-Cryst. Solids 170 (1994) 167.

[48] M. Dimitrova-Pankova, Y. Dimitriev, M. Arnandov, V. Dimitrov, Phys. Chem. Glasses 30 (1989) 260.

[49] K. Itoh, T. Usuki, and S. Tamaki, J. Non-Cryst. Solids, 250–252, 336–39 (1999).

[50] R. S. Kumar and K. Hairiharan, Solid State Ionics, 104, 227–36 (1997).

[51] L. Murawski, C. H. Chung, J. D. Mackenzie, J. Non-Cryst. Solids 32 (1979) 91.

[52] H. Mori, T. Kitami, H. Sakata, J. Non-Cryst. Solids 168 (1994) 157.

[53] H. Mori, J. Igarashi, H. Sakata, Glastech. Ber. 68 (1995) 327.

[54] H. Mori, T. Kitami, H. Sakata, J. Ceram. Soc. Jpn. 101 (1993) 347.

[55] H. Mori, J. Igarashi, H. Sakata, J. Ceram. Soc. Jpn. 101 (1993) 1351.

[56] K. Sega, H. Kasai, H. Sakata, Mater. Chem. Phys. 53 (1998) 28.

[57] H. Sakata, M. Amano, T. Yagi, J. Non-Cryst. Solids 194 (1996) 198.